Evaluation of Diuretic Property of *Argemone mexicana* along with Molecular Docking Study

Pabitra Kumar Sardar [1], Hiron Saraj Devnath[1], Nripendra Nath Biswas[1]*, Bishwajit Bokshi[1]*, Samir Kumar Sadhu[1]

[1] Pharmacy Discipline, Life Science School, Khulna University, Khulna-9208, Bangladesh.

ABSTRACT

Background: Argemone mexicana L. (A. mexicana) has traditionally been used to treat hypertension, urinary issues, and constipation. In this study, we assessed the diuretic activity of the ethanolic crude extract of A. mexicana.

Methods: Phytochemical tests were conducted using standard reagents and methods widely accepted in the field. The diuretic test was performed in metabolic cages using a mouse model, with furosemide (5 mg/kg) as the standard drug. Molecular docking was carried out in PyRx using Autodock Vina 4.2. To assess the stability of the protein-ligand complexes formed during docking, we conducted molecular dynamics (MD) simulations for the β-amyrin-6PZT protein complex and the furosemide-6PZT protein complex. Various parameters, including RMSD, RMSF, Rg, SASA, and hydrogen bonds, were calculated for all protein-ligand complexes.

Results: Phytochemical screening revealed the presence of alkaloids, flavonoids, glycosides, steroids, terpenoids, saponins, and tannins in the crude extract. The crude extract exhibited significant ($p < 0.05$) diuretic activity compared to the control group. Furthermore, we detected the presence of electrolytes (Na+, K+, and Cl-) in the urine of mice treated with the crude extract. In the molecular docking study, among the eighteen compounds studied, β-amyrin displayed superior diuretic potential. The results of the molecular dynamics simulation for the β-amyrin-6PZT protein complex indicated good stability, comparable to the reference drug, furosemide.

Conclusion: The crude extract of A. mexicana demonstrates significant diuretic effects that could be valuable for edema treatment. The findings from the molecular docking and molecular dynamics simulations suggest the potential for further research in developing a novel drug.

Keywords: *Argemone mexicana*, Papaveraceae, Diuretic, Molecular docking, β-amyrin.

1. INTRODUCTION

Many plants are rich sources of various phytochemicals that can be utilized in designing and synthesizing medicines[1]. It is well-established that numerous medicinal plants possess potent diuretic properties, and they are commonly employed in conventional treatments for renal disorders[2-4]. Additionally, the diuretic properties of various plants used in ethnomedicine have been verified through animal studies[5].

Diuretics are medications that enhance the excretion of sodium ions (Na+) and urine production. They find application in the management of various clinical conditions, including hypertension, congestive heart failure, renal failure, and nephrotic syndrome, to regulate the volume and composition of body fluids. Diuretics can also influence the renal regulation of uric acid and the

Corresponding author:
Nripendra Nath Biswas: nnathbiswas@gmail.com
Bishwajit Bokshi: bokshi06@pharm.ku.ac.bd
Received: 19/9/2022 Accepted: 28/4/2023.
DOI: https://doi.org/10.35516/jjps.v16i3.430

levels of various ions such as potassium (K+), hydrogen (H+), calcium (Ca2+), and magnesium (Mg2+), as well as anions like chloride (Cl−), bicarbonate (HCO3−), and dihydrogen phosphate (H2PO4−), in addition to altering Na+ excretion[6].

Diuretics, whether used alone or in combination with other medications, are employed in the treatment of conditions like congestive heart failure, ascites, and pulmonary edema[7-11]. Thiazides and furosemide, two commonly prescribed diuretics, have been associated with several side effects, including electrolyte imbalances, metabolic syndromes, and activation of the renin–angiotensin–neuroendocrine system[7, 10]. Consequently, there is a need for new diuretics with fewer adverse effects, such as those derived from plants, which are generally considered safer.

The Na-K-2Cl cotransporter-1 (NKCC1), also known as 6PZT, is an electroneutral Na+-dependent transporter responsible for the simultaneous transport of Na+, K+, and Cl− ions into cells[12, 13]. In human tissue, 6PZT plays a vital role in regulating cytoplasmic volume, fluid intake, chloride balance, and cell polarity[14-16]. Furosemide and other loop diuretics, frequently used to manage edema and hypertension, inhibit this transporter[17, 18]. Our computer-aided molecular modeling of the binding sites of loop diuretics at 6PZT was prompted by these findings.

A. mexicana L., also known as Ghamoya and a member of the Papaveraceae family, is a rare weed that originated in South America but is now common in many Asian nations, including China and India[19, 20]. The plant is an annual herb, reaching a height of approximately 1 meter; its leaves typically measure 5-11 cm in length and are spiny[21]. The flowers are 4-5 cm in diameter and yellow[22]. Various parts of this plant have been reported to be used in the treatment of conditions such as hypertension, oliguria, diarrhea, ulcers, asthma, and other intestinal afflictions[21, 23-30].

Furthermore, researchers have identified various bioactive compounds in the plant, including alkaloids such as berberine, (+)-reticuline, allocryptopine, (-)-cheilanthifoline, (+)-argenaxine, (+)-higenamine, and N-demethyloxysanguinarine[31, 32], flavonoids, e.g., eriodictyol, isorhamnetin-3-*O*-β-Dglucopyanoside, quercetin, quercetrin, mexitin [33-36], terpenoids, e.g., *trans*-phytol, β-amyrin [32, 34] steroids, e.g., β-sitosterol [37]; miscellaneous, e.g., α-tocopherol, adenosine, adenine, myristic acid, oleic acid, linoleic acid [32, 38], amino acids, e.g., cysteine, phenylalanine[34].

Upon literature survey, based on ethnopharmacological uses of *A. mexicana* in hypertension, oliguria [24], the entire plant was selected for evaluating its diuretic properties in a mouse model. This was followed by a molecular docking and molecular dynamics simulation analysis of the previously reported compounds.

2. MATERIALS AND METHODS

2.1 Collection and identification of *A. mexicana*

The whole plant of *A. mexicana* was collected for this investigation from the Chuknagar area of Jashore, Bangladesh, in January 2017. A voucher specimen of *A. mexicana* was submitted to the Bangladesh National Herbarium in Mirpur, Dhaka (DACB Accession number: 43825) for future reference.

2.2 Drying, grinding, and Cold extraction

The collected whole plants were cleaned and carefully inspected to remove any unwanted objects, other plants, or weeds. They were air-dried for a week. Subsequently, the plant material was ground into a coarse powder using a suitable grinder. The resulting powder was stored in an airtight container, maintaining a cool, dark, and dry environment until the extraction process.

Approximately 800 g of the powdered material was placed in a clean, flat-bottomed glass container and dissolved in 1500 mL of ethanol. The glass container was covered with aluminum foil, and the mixture was allowed to sit for 14 days with intermittent stirring. Afterward, the contents of the glass container were filtered, first through a piece of cotton and then through Whatman® filter paper. The resulting filtrate was subjected to evaporation using a

rotary evaporator, yielding a sticky dark gummy crude extract weighing 18.12 g, with a yield of 2.26%.

2.3 Phytochemical screening

Phytochemical testing was conducted to identify chemical groups present in the test extracts. Various phytochemical experiments on the crude extract were performed using standard techniques[39-43].

2.4 Experimental animal

Swiss-albino mice were sourced from Jahangirnagar University in Savar, Bangladesh, and then raised for one week under standard conditions in the animal lab of the Pharmaceutical Department at Khulna University, Bangladesh. These animals were kept in a natural lighting environment and provided with standard laboratory food and water. The study employed young Swiss albino mice, aged 4-5 weeks, with an average weight of 25-30 g. All procedures adhered to the animal ethical standards established by the Life Science School at Khulna University, Bangladesh (Reference: KUAEC-2018/05/10).

2.5 Acute toxicity study

The acute toxicity assessment was conducted in mice following the recommendations of the Organization for Economic Co-operation and Development (OECD)[44-46]. The crude extract was administered to three groups of mice at doses of 1000, 2000, and 3000 mg/kg, and differences in mortality and body weight were recorded in comparison to a control group. Individual post-dose observations were made during the first 30 minutes, periodically over the first 24 hours, and daily over the subsequent 14 days.

2.6 Diuretic activity evaluation

The diuretic test procedure followed a pre-established methodology adapted by Golla and colleagues with minor modifications[47-50].

In brief, twenty-four mice of both sexes, weighing 27-30 g, were divided into four groups of six each. Each group underwent an 18-hour fasting period without access to food or water before the test. The first group received normal saline (6x2 mL) as a control. The second group (standard) received furosemide (5 mg/kg) as a positive control. The third and fourth groups were administered the crude extract at doses of 200 and 400 mg/kg, respectively. Each group received a total volume of 6 × 2 mL (Vi). Following dosing, the animals were placed in metabolic cages. Throughout the six-hour experiment, the mice were deprived of food and water, and the cages were maintained at a constant temperature of 25.0±0.5 °C. Urinary output (V0) was measured hourly, and the urine was stored at 0–4 °C for later electrolyte measurement. The urinary excretion was estimated using the ratio of urine output (V0) to the total liquid delivered (Vi) (Formula-I). The diuretic action was calculated as the ratio of urinary excretion in the test group (UET) to that in the control group (UEC) (Formula-II). Diuretic activity was determined by the ratio between the diuretic action in the test group (DAT) and that in the control group (Formula-III).

$$\text{Urinary excretion} = \frac{\text{Total urinary output } (V_0)}{\text{Total liquid administered } (V_i)} \times 100 \ldots \text{(I)}$$

$$\text{Diuretic action} = \frac{\text{Urinary excretion of treatment groups}}{\text{Urinary excretion of the control group}} \ldots\ldots\ldots \text{(II)}$$

$$\text{Diuretic activity} = \frac{\text{Diuretic action of test groups}}{\text{Diuretic action of standard group}} \ldots\ldots\ldots \text{(III)}$$

2.7 Analysis of Urine Sample for different cations and anions

The D-50 Series Portable Water Quality Meters from HORIBA Scientific® were employed to measure the pH and conductivity of the preserved urine samples. The concentrations of Na+ and K+ in the samples were determined using a flame photometer, specifically the Janeway Corp. model PFP7. Flame intensity was measured for Na+ and K+ concentrations with appropriate filters, aligning with calibration standards. Results were displayed graphically, and Na+ and K+ concentrations were calculated from the standard curve and expressed in mEq/L[51]. The Cl− content was determined through titration with a 0.05 N silver nitrate solution, utilizing 5% potassium chromate solution as an indicator[52, 53]. To predict the mechanism of action of diuretic drugs, several

indices were calculated for the preserved urine samples, including the saluretic index, natriuretic index (Na+/K+ ratio), kaliuretic index (K+/Na+ ratio), and carbonic anhydrase inhibition (CAI) index.

Here,

$$\text{Saluretic index} = \frac{\text{Urinary excretion of electrolytes in the test group}}{\text{Urinary excretion of electrolytes in the control group}}$$

$$\text{Natriuretic Index} = \frac{\text{Urinary excretion of Sodium ion}}{\text{Urinary excretion of Potassium ion}}$$

$$\text{Kaliuretic index} = \frac{\text{Urinary excretion of Potassium ion}}{\text{Urinary excretion of Sodium ion}}$$

$$\text{CAI index} = \frac{\text{Urinary excretion of Chloride ion}}{\text{Sum of Urinary excretion of Sodium and Potassium ions}}$$

2.8 Molecular docking analysis

Preparation of the ligands

3D structures of already reported eighteen compounds (Figure 1) [22] were retrieved from PubChem (https://pubchem.ncbi.nlm.nih.gov/). PyRx was then used for energy minimization [44].

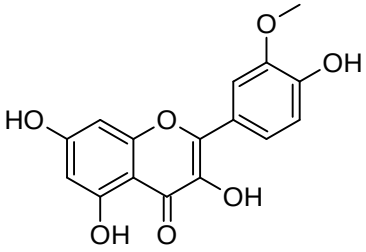

isorhamnetin

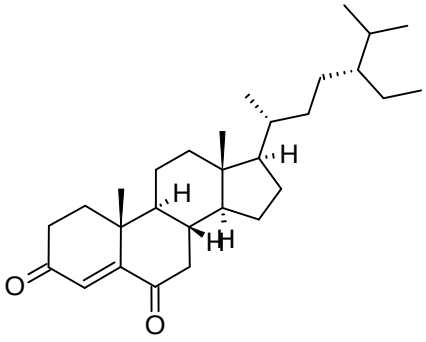

stigmast-4-ene-3,6-dione

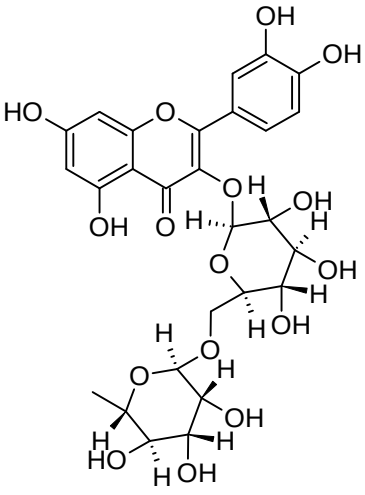

rutin

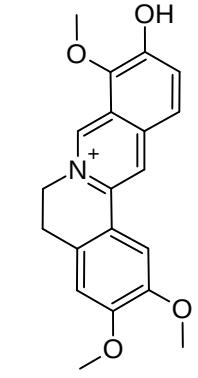

dehydrocorydalmine

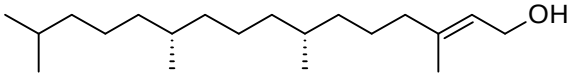

phytol

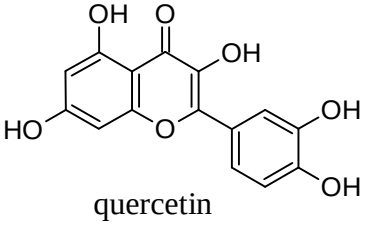

quercetin

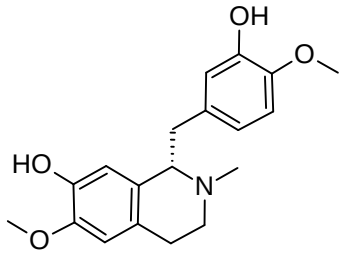

reticuline

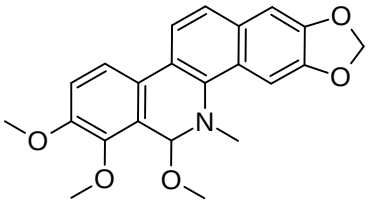

angoline

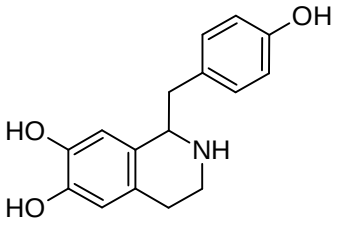

higenamine

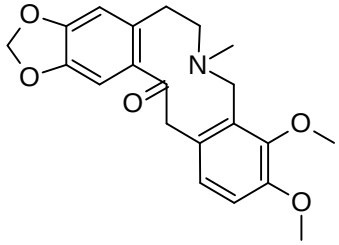

allocryptopine

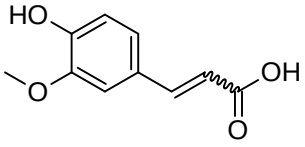

ferulic acid

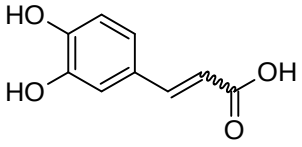

caffeic acid

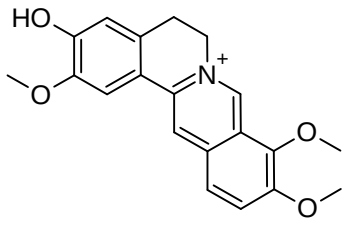

jatrorrhizine

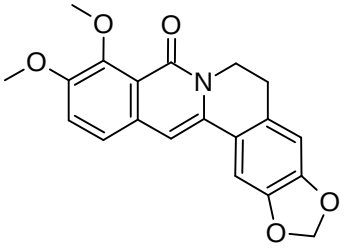

oxyberberine

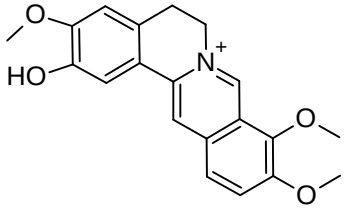

columbamine

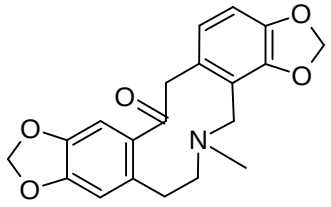

protopine

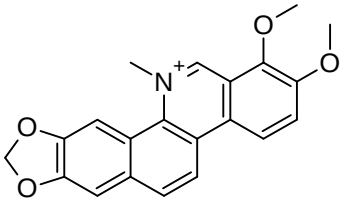

chelerythrine

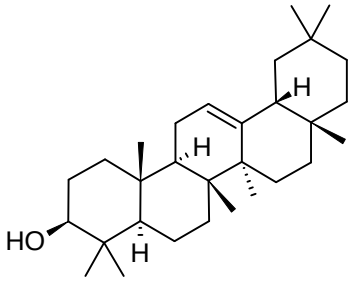

β-amyrin

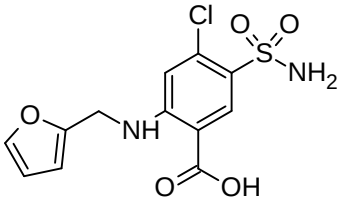

furosemide

Figure 1: Structure of eighteen compounds reported from A. *mexicana* and furosemide.

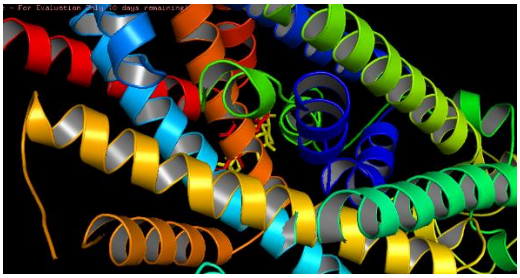

Figure 2: Binding region of docked furosemide (red) and β-amyrin (yellow) with 6PZT protein.

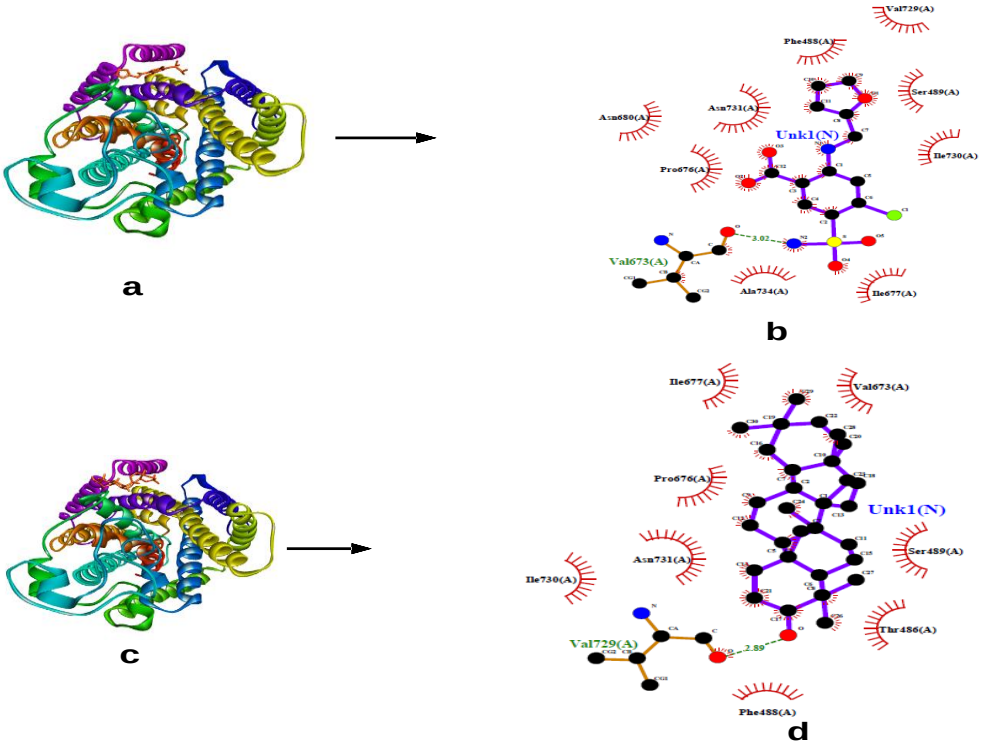

Figure 3: (a) Furosemide and (c) β-amyrin protein complex with 6PZT; (b) furosemide and (d) β-amyrin 2D interaction.

β-amyrin-6PZT protein complex

furosemide -6PZT complex

apo-protein

Preparation of the protein

The 6PZT protein was obtained from the Protein Data Bank (https://www.rcsb.org). Using Discovery Studio Visualizer, the retrieved protein underwent cleaning, and

polar hydrogen atoms were added. Since 6PZT forms a dimer with two-fold symmetry, we considered a single chain for docking[54]. Additionally, SwissPDB Viewer was utilized for energy minimization[55].

Molecular docking and visualization

Amino acid residues were selected for docking using AutoDock Vina 4.2 in PyRx[56]. The grid box was maximized to cover the entire protein. LigPlot Plus 2.2.4 was employed to analyze the outcomes. Through molecular docking, we identified interactive amino acids with the target proteins and determined the binding affinities of the selected drugs.

Molecular dynamics simulations

GROMACS 2021 was utilized in simulations of molecular dynamics (MD) using the charmm36 force field[57, 58]. The ligands parameters were generated using the CGenFF server for CHARMM General (cgnff.umaryland.edu)[59]. A decahedron box with a TIP3P water model was used to dissolve protein-ligand complexes. The system was neutralized by the use of Na^+ and Cl^- ions. Following minimization, the system was run with coupled temperature and pressure control using the NVT and NPT ensemble at 310 K and 1 bar. The final MD run lasted 100 nanoseconds. To assess relative stability, root mean square deviation (RMSD), root mean square fluctuations (RMSF), radius of gyration (Rg), solvent-accessible surface area (SASA), and hydrogen bond analyses were performed.

2.9 Statistical Analysis

Data were analyzed using Student's unpaired t-test in GraphPad Prism Version 5.03, and the results were presented as Mean ± Standard Error of Mean (S.E.M) (GraphPad Software, San Diego, CA, USA). All in vivo study outcomes were compared with those of the control group, and a significance level of $P < 0.05$ was applied.

3. RESULT

3.1 Preliminary phytochemical study

This study consisted of testing several chemical groups found in the extract. The outcome of the phytochemical study of the crude extract is summarized in **Table 1**.

Table 1: Results of phytochemical study of *A. mexicana* crude extract

Phytochemical groups	Results
Reducing sugars	−
Tannins	+
Flavonoids	+
Saponins	+
Steroids	+
Alkaloids	+
Glycosides	+
Terpenoids	+
Acidic compounds	+

Here, + indicates Presence; − indicates Absence

3.2 Acute toxicity study

This investigation provided evidence of the extract's non-toxicity. None of the doses used resulted in fatalities or adverse responses until the end of the trial period, suggesting that the LD50 of the extract may exceed 3000 mg/kg.

3.3 Diuretic activity test

The different parameters for assessing diuretic activity

in the extract, control, and standard groups are presented in Tables 2, 3, and 4. Table 2 displays information on urine volume, urinary excretion, diuretic action, and diuretic activity. Table 3 presents data on the diuretic index, pH, and conductivity, while Table 4 provides information on the electrolyte concentrations (Na+, K+, Cl−) in mEq/L, saluretic index, Na+/K+ ratio, and CAI in the urine of animals treated with the extract, furosemide, and untreated control groups.

Table 2: Effects of *A. mexicana* crude extract on volume of urine, urinary excretion, diuretic action and diuretic activity in mice

Group	Cumulative urine volume (V_0 mL) after 6h	Urinary excretion {(V_0/V_i) X 100}	Diuretic action (U_{ET}/U_{EC})	Diuretic activity (D_{AT}/D_{AF})
Control (Normal Saline)	3.35±0.15	27.91	1.00	–
Furosemide (5 mg/kg)	5.1±0.10[b]	42.50	1.52	1.00
Crude Extract (200 mg/kg)	3.85±0.25	32.08	1.14	0.75
Crude Extract (400 mg/kg)	4.9±0.80[a]	40.83	1.46	0.96

Values are expressed as Mean ± S.E.M; n = 6; [a]$P < 0.05$, [b]$P < 0.001$, compared to the control group

Table 3: Effects of *A. mexicana* crude extract and furosemide on urinary volume, diuretic index, conductivity and pH in mice

Group	Diuretic Index	pH	Conductivity (mS/cm)
Control (Normal Saline)	1	7.14 ± 0.02	6.05 ± 0.45
Furosemide (5 mg/kg)	1.52	7.36 ± 0.04[b]	16.77 ± 0.02[c]
Crude extract (200 mg/kg)	1.14	7.05 ± 0.03	15.74 ± 0.01[b]
Crude extract (400 mg/kg)	1.46	7.79 ± 0.04[b]	11.59 ± 0.05[b]

Values are expressed as Mean±S.E.M; n = 6; Diuretic index = Urine volume of test group/ Urine volume of control group; [a]$P < 0.05$. [b]$P < 0.01$, [c]$P < 0.001$, compared to the control group (Student's unpaired *t*-test).

Table 4: Effect of the crude extract and furosemide on urinary electrolytes excretion in mice

Group	Cumulative Concentrations of ions (mEq/L/6h)			Saluretic Index			Na^+ / K^+	K^+/ Na^+	CAI {Cl^-/ (Na^+ + K^+)}
	Na^+	K^+	Cl^-	Na^+	K^+	Cl^-			
Control (Normal Saline)	49.5±6.13	29.5±0.74	63.3±3.63	–	–	–	1.67	0.59	0.80
Furosemide (5 mg/kg)	134.4±6.13[c]	53.4±1.47[c]	78.3±2.20[b]	2.71	1.81	1.23	2.51	0.39	0.41
Crude Extract (200 mg/kg)	187.5±6.13[b]	36.3±1.54[a]	91.7±2.20[a]	3.79	1.23	1.44	5.17	0.19	0.40
Crude Extract (400 mg/kg)	215.8±9.36[b]	73.2±1.29[b]	95.0±1.44[b]	4.36	2.48	1.50	2.94	0.33	0.32

Values are expressed as Mean ± S.E.M; n = 6; [a]$P < 0.05$, [b]$P < 0.01$; [c]$P < 0.001$; compared with the control group (Student's unpaired *t*-test).

3.4 Effect on urine volume, pH, and conductivity

The urine volume for both doses (200 and 400 mg/kg) of the crude extract (3.85 ml, 4.90 ml) was found to be higher compared to the control (3.35 ml) (Table 2).

The pH of the urine increased dose-dependently at both doses for the crude extract (7.05, 7.79) compared to the control (7.14) (Table 3). Additionally, specific conductivity was enhanced by the crude extract (15.74, 11.59) compared with the control (6.05) (Table 3).

3.5 Effects on electrolyte excretion

Our findings demonstrated that the excretion of Na+ (measured in mEq/L) from the crude extracts increased at both 200 and 400 mg/kg (187.5, 215.8). Furthermore, an increase in the excretion of potassium ions was observed for the crude extracts (36.3, 73.2) at both 200 and 400 mg/kg. Additionally, an elevation in the excretion of chloride ions at both 200 and 400 mg/kg for the crude extracts (91.7, 95.00) was found (Table 4). The saluretic index, natriuretic index, kaliuretic index, and CAI index increased dose-dependently for the crude extract (Table 4).

3.6 Molecular docking analysis

β-Amyrin displayed a superior binding affinity (-8 kcal/mol) with the protein compared to the standard furosemide (-5.8 kcal/mol). Additionally, other compounds such as protopine, both chelerythrine and Stigmast-4-ene-3,6-dione, rutin, and angoline also exhibited better binding affinities of 7.7, 7.3, 7.2, and 7.1 kcal/mol, respectively (Table 5).

Table 5: Docking results of the selected reported ligand compounds with 6PZT protein

Compounds Name	Binding Affinity (kcal/mol)	Interacting amino acids
Isorhamnetin	−6.6	Phe488, Val729, Ala492, Ile730, Pro676, Ser489, Asn731, Asn672, Ala734
Stigmast-4-ene-3,6-dione	**−7.3**	Ile324, Leu531, Thr530, Met325, Val534, Val321, Thr328, Leu527, Ile526, Thr332, Leu523
Rutin	**−7.2**	Ile677, Asn731, Val673, Val729, Pro676, Ile730, Thr486, Ile493, Asn672, Ser489
Dehydrocorydalmine	−6.5	Ile677, Val673, Asn731, Ile730, Pro676, Phe488, Ala492, Thr486, Ser489, Val729, Glu484
Phytol	−5.4	Phe488, Val729, Ile730, Ala492, Ser489, Pro676, Asn731, Asn672, Ala734, Trp733,Val673,Ile677, Phe681, Asn680
Quercetin	−6.8	Glu484, Ile493, Asn672, Glu485, Pro676, Asn680, Ile730, Asn731, Ile677, Ala734
Reticuline	−6.3	Ser489, Ile493, Asn672, Glu485, Pro676, Asn731, Ile677, Ala734, Asn680, Phe681
Angoline	**−7.1**	Ser489, Asn731, Pro676, Ile730, Val673, Ala734, Trp733, Ile677, Asn680
Higenamine	−6.4	Asn672, Val673, Asn731, Glu485, Pro676, Ser489, Ile730, Phe488, Thr486
Allocryptopine	**−7**	Ile677, Asn731, Pro676, Ile730, Thr486, Phe488, Ser489, Val729
Ferulic acid	−5.1	Phe488, Ser489, Asn731, Ile730, Pro676, Ile677, Asn680, Ala734, Val673
Caffeic acid	−5.1	Ala434, Leu612, Ser613, Leu438, Gln435, Leu297, Arg294
Jatrorrhizine	−6.7	Gly664, Phe665, Trp733, Ile677, Asn731, Pro676, Ala734, Asn680
Oxyberberine	−6.9	Ile677, Ile668, Trp733, Val673, Asn731, Pro676, Ser489
Columbamine	−6.1	Leu523, Leu527, Thr332, Thr328, Val321, Val534, Thr530
Protopine	**−7.7**	Ile677, Pro676, Asn731, Phe488, Ile730, Ser489, Val729, Thr486
Chelerythrine	**−7.3**	Ala734, Ile677, Asn680, Asn731, Pro676, Ala492, Ile730
β-Amyrin	**−8**	Ile677, Val673, Pro676, Asn731, Ser489, Ile730, Thr486, Val729, Phe488
Furosemide	−5.8	Val729, Phe488, Ser489, Asn731, Asn680, Ile730, Pro676, Val673, Ala734, Ile677

Compounds marked bold indicated the better binding affinities.

3.7 Molecular dynamics simulation

RMSD considers deviations between two three-dimensional structures over time[60]. Over the course of 100 ns, we analyzed the RMSD of backbone atoms in the apo-protein, furosemide-protein complex, and β-amyrin-protein complex to assess the stability of all systems (Figure 4a).

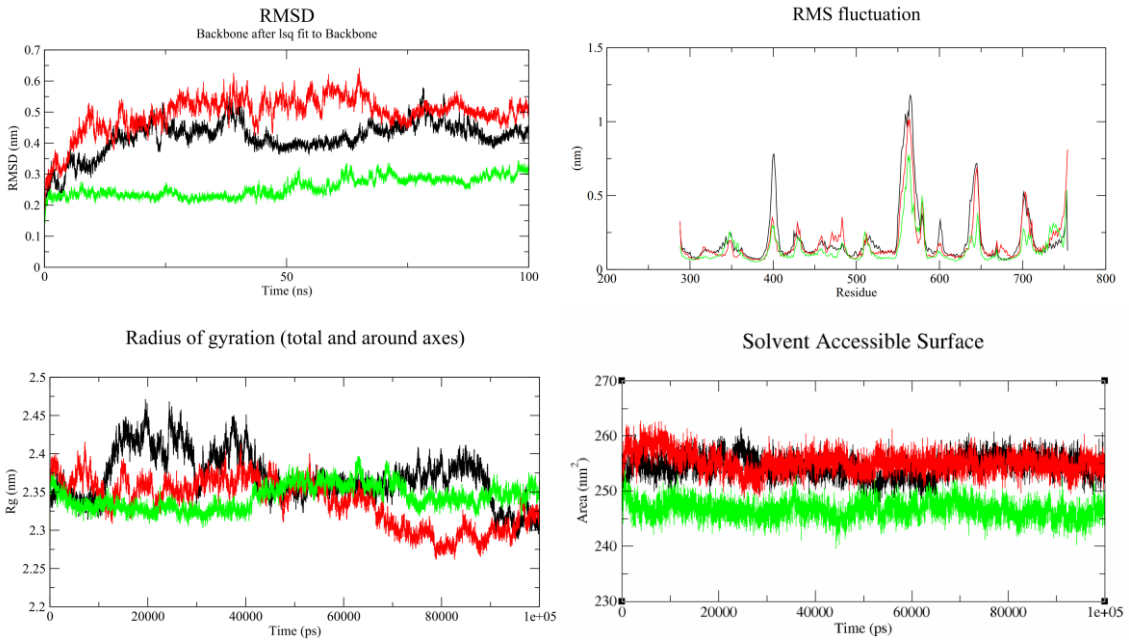

Figure 4: a) Plot of RMSD of backbone atoms vs. time (in nano seconds), b) RMSF of backbone atoms versus residue number, c) Radius of gyration (Rg) versus time (in pico seconds), d) solvent accessible surface area (SASA) versus time (in pico seconds) for β-amyrin-6PZT protein complex (black), furosemide -6PZT complex (red), and for apo-protein (green)

In the initial 20 ns, structural rearrangements were followed by minor conformational alterations in all systems. Apoprotein underwent multiple conformational changes throughout the investigation. The RMSD value of the β-amyrin-protein complex fluctuated between 0.0005 and 0.58 nm, with an average value of 0.42 nm and no significant spikes, indicating that β-amyrin effectively stabilized the protein by binding to it. In contrast, the furosemide-protein complex exhibited a steadily increasing trend in RMSD.

Regarding the overall RMSD for all systems, the apo-protein fluctuated within the range of 0.006-0.34 nm, with an average RMSD of 0.26 nm. On the other hand, the RMSD of the β-amyrin-protein complex and the furosemide-protein complex ranged from 0.0005 nm up to 0.42 nm and 0.50 nm, respectively. Our comprehensive RMSD analysis suggests that β-amyrin is more effective than furosemide in stabilizing the protein.

RMSF is the fluctuations observed in residues or atoms present in a macromolecule[61]. In this study, we assessed the RMSF of backbone residues in both the apo-protein and all protein-ligand complexes (Figure 4b). Even in regions experiencing the most significant changes, the RMSF graphs exhibited a similar profile, with average RMSF values of 0.21 nm for the β-amyrin-protein complex and 0.18 nm for the furosemide-protein complex.

However, our RMSF analysis indicated that the β-amyrin-protein complex stabilizes the protein in a manner similar to that of the furosemide-protein complex.

Rg is a routinely used parameter to predict the compactness of macromolecules[62]. In this study, we analyzed the Rg of the apo-protein and all protein-ligand complexes (Figure 4c). The β-amyrin-protein complex exhibited a higher Rg until 40 ns, after which it showed a lower Rg, indicating stability. However, the average Rg value of the β-amyrin-protein complex was 2.36 nm, which was comparable to that of the furosemide-protein complex (average Rg value = 2.34 nm).

A molecule's surface area that interacts with the solvent molecules is its solvent-accessible surface area [63]. The β-amyrin-protein complex and the furosemide-protein complex had average SASA values of 254.54 nm^2 and 255.21 nm^2, respectively (Figure 4d). Based on the SASA values for all complexes, it appeared that the furosemide-protein complex was more exposed to water solvent than the β-amyrin-protein complex. Our results indicate that the protein coupled with β-amyrin was highly stable and compact.

Number of hydrogen bonds

Hydrogen bond interactions play a crucial role in stabilizing macromolecules and are directly related to binding affinity and drug efficacy[64, 65]. Figure 5 illustrates the number of hydrogen bonds formed during the 100 ns simulation run as a result of interactions between the protein and ligand combinations. Based on our hydrogen bond observations, all compounds maintained optimized hydrogen bonding for up to 25 ns. This suggests that the chemical can have the necessary impact on drug specificity, metabolism, and adsorption.

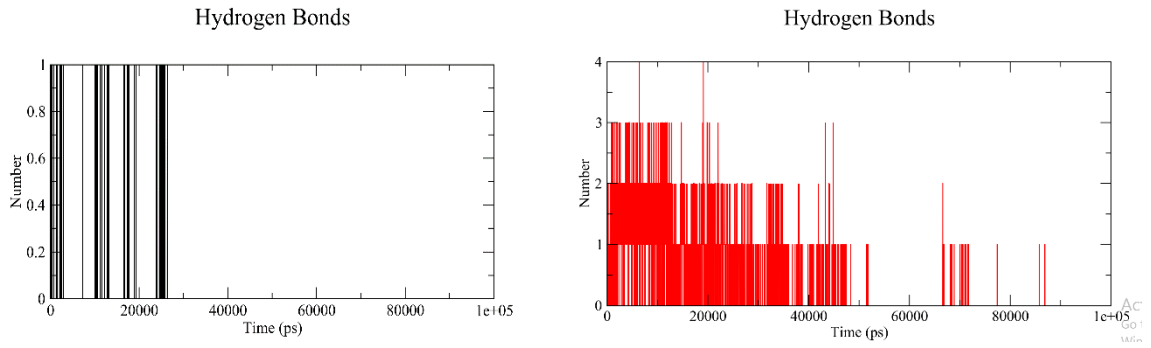

Figure 5: Plot of Number of hydrogen bonds versus time (in picoseconds) for β-amyrin-6PZT protein complex (black), furosemide -6PZT protein complex (red)

4. DISCUSSION

The phytochemical tests conducted on the extract revealed the presence of several important constituents, including tannins, flavonoids, glycosides, saponins, steroids, etc. Previous studies have shown that these types of phytochemicals are responsible for diuretic activity [66, 67]. Therefore, these compounds may be responsible for the traditional medicinal uses associated with diuretic activity. Consequently, further studies targeting the assessment of the diuretic potential of the plant were conducted.

The current study aimed to assess the diuretic properties of the extract. Two key indicators of diuresis are an increase in net urinary volume and elevated excretion of electrolytes in the urine[9]. These processes result from the inhibition of water and electrolyte reabsorption into the circulation in the renal tubules. Thiazide diuretics restrict the Na^+/Cl^- symporter (co-transporter system) in the distal tubule by competing for the Cl^- binding site, while the standard loop diuretic drug, furosemide, increases urinary Na^+ excretion by inhibiting the $Na^+/K^+/Cl^-$

symporter in the thick ascending limb of the loop of Henle[9]. Therefore, in this study, both urine volume and electrolyte concentrations were evaluated to assess the diuretic effect of the A. mexicana crude extract. In the current investigation, a dose of 5 mg/kg of furosemide produced significant diuresis in mice for 6 hours. Our findings indicate that the extract increased urine volume and urinary excretion (Table 2). We observed a notable and significant increase in the excretion of Na+, K+, and Cl− compared to the control group, similar to what was observed with furosemide (Table 3). Additionally, the extract exhibited a progressive increase in electrolyte excretion (Na+, K+, and Cl−) in a dose-dependent manner (Table 4).

A saluretic activity metric was defined as the amount of Na+, K+, and Cl− excretion[68]. The extract exhibited dose-dependent electrolyte and water excretion to varying degrees. To assess natriuretic activity, the ratio of Na+ to K+ was calculated[69, 70]. Values greater than 2.0 indicate a beneficial natriuretic effect, while ratios greater than 10.0 suggest a potassium-sparing effect[71]. The Na+/K+ values (Table 4) for the crude extract at their respective doses of 200 and 400 mg/kg were 2.94 and 5.17, respectively. This result falls within the acceptable value range of 2, suggesting that the extract possesses a potent natriuretic effect.

Previous studies have reported that several bioactive compounds contribute to the diuretic effect, including flavonoids, saponins, triterpenoids[70, 72-74] glycosides [66, 70, 75], tannins [70, 72] and steroids [67]. These phytochemicals may induce the diuretic effect by stimulating regional blood flow, initial vasodilation, inhibiting water and electrolyte reabsorption by tubules, or enhancing renal circulation, ultimately leading to diuresis[76]. The preliminary phytochemical study of the extract confirmed the presence of the aforementioned phytochemicals. Therefore, it can be inferred that these phytochemicals, alone or in combination, may be responsible for the diuretic activity of the plant. Additionally, compounds such as quercetin[77], caffeic acid [78], and rutin [79] present in the plant, have been reported to exhibit diuretic activities. These compounds could contribute to the diuretic properties of the A. mexicana crude extract.

The human cation–chloride cotransporter NKCC1 is the target protein for the standard drug Furosemide. Inhibiting this cotransporter is the mechanism of action for loop diuretics[54]. Therefore, the activity of the test ligands was assessed against this cotransporter protein and compared with the standard, Furosemide. Among the previously reported compounds from this plant, β-Amyrin, a triterpene alcohol, displayed a binding affinity of −8 kcal/mol, which is almost 1.4 times greater than that of Furosemide (−5.8 kcal/mol) (Table 5), and the binding site of these two compounds is identical, as shown in Figure 2. While the standard drug Furosemide interacted with amino acids Phe488, Ser489, Val673, Pro676, Ile677, Asn680, Val729, Ile730, Asn731, and Ala734, β-amyrin interacted with amino acids Thr386, Phe488, Ser489, Val673, Pro676, Ile677, Val729, Ile730, and Asn731. Amino acids Phe488, Ser489, Val673, Pro676, Ile677, Val729, Ile730, and Asn731 are common to both compounds (Figure 3). Furosemide formed a hydrogen bond with the Val673 amino acid, and β-amyrin formed a hydrogen bond with Val729. Hydrogen bonding is crucial for protein stabilization as it maintains specific shapes. Here, the presence of the hydrogen bond indicates the stable protein complex of β-amyrin with 6PZT. Other amino acids, such as Phe488, Ser489, Pro676, Ile677, Ile730, and Asn731, all formed hydrophobic interactions with the protein. Therefore, β-amyrin could also play a role in diuretic activity. Our literature findings also revealed that terpenoid-enriched plant extracts promote diuresis, which supports this result[74].

5. CONCLUSION

The results of in vivo studies on diuretic activity support the ethnopharmacological use of A. mexicana for treating urinary problems. In the molecular docking study, among the eighteen reported compounds, β-amyrin, a

triterpene alcohol, exhibited superior diuretic potential. RMSD, RMSF, Rg, hydrogen bonds, and energy analysis all demonstrated the stable binding of the β-amyrin-6PZT protein complex. This stable binding supports the diuretic activity of Argemone mexicana. Therefore, this evidence can be utilized for discovering the mechanism of action and investigating the pharmacodynamic and pharmacokinetic parameters.

Declaration of interest

None.

Consent for publication

All co-authors have consented to the publication of this manuscript.

Availability of data and materials

The datasets supporting the conclusions of this article are included within the article.

Funding

The project was not supported by any funding.

REFERENCES

1. Bhowmik, A. K., Cabral, P., Cyclone Sidr impacts on the Sundarbans floristic diversity. *Earth Science Research.* **2013;** 2(2): 62.
2. Maksimović, Z., Dobrić, S., Kovačević, N., Milovanović, Z., Diuretic activity of Maydis stigma extract in rats. *Die Pharmazie-An International Journal of Pharmaceutical Sciences.* **2004;** 59(12): 967-971.
3. Tanira, M., Ageel, A., Al-Said, M., A study on some Saudi medicinal plants used as diuretics in traditional medicine. *Fitoterapia.* 1989; 60 (5): 443-447.
4. Rahhal, B., Taha, I., Najajreh, I., Basha, W., Alzabadeh, H., Zyoud, A., Sharaga, A., Alratrout, Z., Yunis, N., Kanaan, O. and Raddad, J., Phytochemical Screening and Diuretic Activity of selected Palestinian Medicinal plants in Mice using an Aqueous Extract Division of Physiology, Pharmacology and Toxicology. *Jordan Journal of Pharmaceutical Sciences*. 2023; 16(2): 467-467.
5. Benjumea, D., Abdala, S., Hernandez-Luis, F., Pérez-Paz, P., Martin-Herrera, D., Diuretic activity of Artemisia thuscula, an endemic canary species. *Journal of Ethnopharmacology*. 2005; 100 (1-2): 205-209.
6. Brunton L, B. D., Buxton I, Parker K, *The Goodman and Gilman's Manual of Pharmacology and Therapeutics.* McGraw Hill Companies, Inc: New York, 2008; 475-498.
7. Gupta, S., Neyses, L., Diuretic usage in heart failure: a continuing conundrum in 2005. *European heart journal.* 2005; 26 (7): 644-649.
8. Hughes, A. D., How do thiazide and thiazide-like diuretics lower blood pressure? *Journal of the Renin-Angiotensin-Aldosterone System.* 2004; 5(4): 155-160.
9. Jackson, E. K., Drugs affecting renal and cardiovascular function. *Goodman & Gilman's the pharmacological basis of therapeutics, McGraw-Hill Professional, New York.* 2006; 737.
10. Morganti, A., Should a diuretic always be the first choice in patients with essential hypertension? The case for no. *Journal of the American Society of Nephrology*. 2005; 16 (3 suppl 1), S70-S73.
11. O'Brien, J. G., Chennubhotla, S. A., Chennubhotal, R. V., Treatment of edema. *American family physician.* 2005; 71 (11): 2111-2117.
12. Haas, M., The na-k-cl cotransporters. *American Journal of Physiology-Cell Physiology* **1994,** *267* (4), C869-C885.
13. Hebert, S. C.; Mount, D. B.; Gamba, G., Molecular physiology of cation-coupled Cl− cotransport: the SLC12 family. *Pflügers Archiv.* 2004; 447 (5): 580-593.

14. Delpire, E., Wolfe, L., Flores, B., Koumangoye, R., Schornak, C. C., Omer, S., Pusey, B., Lau, C., Markello, T., Adams, D. R., A patient with multisystem dysfunction carries a truncation mutation in human SLC12A2, the gene encoding the Na-K-2Cl cotransporter, NKCC1. *Molecular Case Studies.* 2016; 2(6): a001289.
15. Macnamara, E. F., Koehler, A. E., D'Souza, P., Estwick, T., Lee, P., Vezina, G., Network, U. D., Fauni, H., Braddock, S. R., Torti, E., Kilquist syndrome: a novel syndromic hearing loss disorder caused by homozygous deletion of SLC12A2. *Human mutation.* 2019; 40(5): 532-538.
16. Moseng, M. A., Su, C.-C., Rios, K., Cui, M., Lyu, M., Glaza, P., Klenotic, P. A., Delpire, E., Yu, E. W., Inhibition mechanism of NKCC1 involves the carboxyl terminus and long-range conformational coupling. *Science Advances.* 2022; 8(43): eabq0952.
17. Hannaert, P., Alvarez-Guerra, M., Pirot, D., Nazaret, C., Garay, R., Rat NKCC2/NKCC1 cotransporter selectivity for loop diuretic drugs. *Naunyn-Schmiedeberg's archives of pharmacology*. 2002; 365(3): 193-199.
18. Zhao, Y., Roy, K., Vidossich, P., Cancedda, L., De Vivo, M., Forbush, B., Cao, E., Structural basis for inhibition of the Cation-chloride cotransporter NKCC1 by the diuretic drug bumetanide. *Nature communications.* 2022; 13(1): 1-12.
19. Bhalke, R., Gosavi, S., Anti-stress and antiallergic effect of Argemone mexicana stems in asthma. *Arch Pharm Sci Res*. 2009; 1(1): 127-129.
20. Elizondo-Luévano, J. H., Castro-Ríos, R., López-Abán, J., Gorgojo-Galindo, O., Fernández-Soto, P., Vicente, B., Muro, A., Chávez-Montes, A., Berberine: A nematocidal alkaloid from Argemone mexicana against Strongyloides venezuelensis. *Experimental Parasitology*, 2021; 220: 108043.
21. Chopra, R. N., Glossary of Indian medicinal plants. 1956.
22. Brahmachari, G., Gorai, D., Roy, R., Argemone mexicana: chemical and pharmacological aspects. *Revista Brasileira de Farmacognosia*, 2013; 23: 559-567.
23. Agra, M. d. F., Baracho, G. S., Nurit, K., Basílio, I. J. L. D., Coelho, V., Medicinal and poisonous diversity of the flora of "Cariri Paraibano", Brazil. *Journal of ethnopharmacology*. 2007; 111(2): 383-395.
24. Bieski, I. G. C., Rios Santos, F., de Oliveira, R. M., Espinosa, M. M., Macedo, M.; Albuquerque, U. P., de Oliveira Martins, D. T., Ethnopharmacology of medicinal plants of the pantanal region (Mato Grosso, Brazil). *Evidence-Based Complementary and Alternative Medicine.* 2012: 2012.
25. Bose, B., Vijayvargiya, R., Saifi, A., Sharma, S., Chemical and pharmacological studies on Argemone mexicana. *Journal of Pharmaceutical Sciences*. 1963; 52(12): 1172-1175.
26. Ambasta, S. S., *The useful plants of India*. Publications & Information Directorate: 1986.
27. Prajapati, N. D., Purohit, S., Sharma, A. K., Kumar, T., A handbook of medicinal plants: A complete source book. In *A handbook of medicinal plants: a complete source book*. 2003; 554-554.
28. 28. Savithramma, N., Sulochana, C., Rao, K., Ethnobotanical survey of plants used to treat asthma in Andhra Pradesh, India. *Journal of Ethnopharmacology*. 2007; 113(1): 54-61.
29. Sarkar, K. K., Mitra, T., Acharyya, R. N., Sadhu, S. K., Phytochemical screening and evaluation of the pharmacological activities of ethanolic extract of Argemone mexicana Linn. aerial parts. *Oriental Pharmacy and Experimental Medicine.* 2019; 19(1): 91-106.
30. Alam, A., Khan, A. A., Argemone mexicana L.: A weed with versatile medicinal and pharmacological applications. *Ann. Phytomed. Int. J*. 2020; 9: 218-223.
31. Israilov, I., Yuhusov, M., Alkaloids of four Agremone species. *Khim Prir Soedin*. 1986; 2: 204-206.
32. Chang, Y. C., Chang, F. R., Khalil, A. T., Hsieh, P. W., Wu, Y.C., Cytotoxic benzophenanthridine and benzylisoquinoline alkaloids from Argemone mexicana. *Zeitschrift für Naturforschung C*. 2003; 58 (7-8): 521-526.

33. Harborne, J. B., Williams, C. A., Flavonoids in the seeds of Argemone mexicana: a reappraisal. *Phytochemistry*. 1983; 22(6): 1520-1521.
34. Sukumar, D., Arivudai Nambi, R., Sulochana, N., Studies on the leaves of Argemone mexicana. *Fitoterapia*. 1984.
35. Singh, S., Singh, T. D., Pandey, V., Constituents of Argemone species. *Journal of the Indian Chemical Society*. 2011; 88(2): 275-276.
36. Singh, S., Pandey, V. B., Singh, T. D., Alkaloids and flavonoids of Argemone mexicana. *Natural product research*. 2012; 26(1): 16-21.
37. Pathak, N. R., Biswas, M., Seth, K., Dwivedi, S. D., Pandey, V., Chemical investigation of Argemone mexicana. *Pharmazie*. 1985; 40(3).
38. Badami, R., Gunstone, F., Vegetable oils. X.—Examination of component acids of Argemone mexicana seed oil by reversed-phase chromatography. *Journal of the Science of Food and Agriculture*. 1962; 13(4): 255-257.
39. Paul, P. P., Kundu, P., Karmakar, U. K., Chemical and Biological Investigation of Sanchezia nobilis Leaves Extract. *Jordan Journal of Pharmaceutical Sciences*. 2022; 15(1): 121-131.
40. Kundu, P., Debnath, S. L., Sadhu, S. K., Exploration of Pharmacological and Toxicological Properties of Aerial Parts of Blumea lacera, a Common Weed in Bangladesh. *Clinical Complementary Medicine and Pharmacology*. 2022; 2(3): 100038.
41. Karmakar, U. K., Akter, S., Bokshi, B., Sadhu, S. K., Exploration of Analgesic, Antiinflammatory, Laxative, and Anthelmintic Activities of Hygrophila phlomoides. *Int. J. Pharm. Sci. Rev. Res. 77*(2): 38-43.
42. Ahad, M. F., Zilani, M. N. H., Akter, A., Md, A. S., Nasrullah, U. K. K., Biswas, N. N., Anisuzzman, M., Bokshi, B., Comparative Pharmacological Potential of Ceriops decandra (Griff.) and Ceriops tagal Linn: Medicinal Plants of the Sundarbans. *Journal of Medicinal Plants*. 2021; 9(4): 14-23.
43. Uddin, A. S., Ahmed, M. I., Karmakar, U. K., Biswas, N. N., Bokshi, B., Sadhu, S. K., Evaluation of Pharmacological Potentialities of Polar and Nonpolar Fractions of Justicia aurea Extract. *Int. J. Pharm. Sci. Rev. Res.* 77(1); 60-64.
44. Medha, M. M., Devnath, H. S., Biswas, B., Bokshi, B., Sadhu, S. K., In silico profiling of analgesic and antihyperglycemic effects of ethanolic leaves extract of Amischotolype mollissima: evidence from in vivo studies. *Saudi Journal of Biological Sciences*. 2022; 103312.
45. Uddin, A. S., Mondal, B., Ramproshad, S., Anisuzzman, M., Bokshi, B., Sadhu, S. K., Phytochemical Screening and Pharmacological Assessment of Justicia aurea Grown in Bangladesh. *Int. J. Pharm. Sci. Rev. Res.* 75(2): 130-134.
46. Al-Awar, M.S.A., Acute and Sub-Acute Oral Toxicity Assessment of Mixed Extract of Trigonella Foenum-Graecum Seeds and Withania Somnifera Root in Rats. *Jordan Journal of Pharmaceutical Sciences*. 2022; 15(4): 493-506.
47. Golla, U., Gajam, P. K., Bhimathati, S. S., Evaluation of diuretic and laxative activity of hydro-alcoholic extract of Desmostachya bipinnata (L.) Stapf in rats. *Journal of integrative medicine*. 2014; 12(4): 372-378.
48. Islam, M., Hasan, M., Dey, A., Bokshi, B., Das, A. K., Sadhu, S. K., Biswas, N. N., Identification of Potential Diuretic and Laxative Drug Candidates from Avicennia officinalis L. Bark through In Vivo Mice Model Studies and In Vitro Gas Chromatography-Mass Spectrometry and Molecular Docking Analysis. *Evidence-based Complementary & Alternative Medicine (eCAM)*. 2022, 2022.
49. Islam, M. N., Hossen, M. K., Joardar, J. C., Bokshi, B., Das, A. K., Sadhu, S. K., Biswas, N. N., Diuretic and laxative activities of Moringa oleifera seeds and pods in mice. *Khulna University Studies*. 2020; 31-39.

50. Sultana, M. S., Golder, M., Biswas, B., Karmakar, U. K., Bokshi, B., Alam, M. J., Shahriar, M., Sadhu, S. K., Antioxidative and Antidiabetic Potentials of the Pneumatophores of Heritiera fomes Buch. Ham. *Dhaka University Journal of Pharmaceutical Sciences.* 2022; 283-291.
51. Vogel, A. I.. Jeffery, G. H., *Vogel's textbook of quantitative chemical analysis*. Wiley: 1989.
52. Beckette AH, S. J., *Practical pharmaceutical chemistry, Part-I.* 4th Edition ed.; Athlone Press: London, 1988.
53. Sarker, M., Ahmed, T., Islam, M. N., Biswas, B., Dev, S., Bokshi, B., Das, A. K., Nath, N., Diuretic and laxative activities of Kandelia candel and Brownlowia tersa in experimental mice. *Journal of Medicinal Plants*. 2021; 9(2): 59-65.
54. Yang, X., Wang, Q., Cao, E., Structure of the human cation–chloride cotransporter NKCC1 determined by single-particle electron cryo-microscopy. *Nature Communications.* 2020; 11(1): 1016.
55. Devnath, H. S., Ahmed, M. I., Medha, M. M., Islam, M. N., Biswas, R. P., Islam, M. A., Sadhu, S. K., HPLC Analysis and Antimicrobial, Antidiarrheal and Antihyperglycemic Properties of Eurya acuminata along with in silico Profiles. *Phytomedicine Plus*. 2022; 2(3): 100291.
56. Dallakyan, S., Olson, A. J., Small-molecule library screening by docking with PyRx. In *Chemical biology*, Springer; 2015: 243-250.
57. Berendsen, H. J., van der Spoel, D., van Drunen, R., GROMACS: A message-passing parallel molecular dynamics implementation. *Computer physics communications*. 1995; 91(1-3): 43-56.
58. Vermaas, J. V., Hardy, D. J., Stone, J. E., Tajkhorshid, E., Kohlmeyer, A., TopoGromacs: Automated topology conversion from CHARMM to GROMACS within VMD. ACS Publications: 2016.
59. Vanommeslaeghe, K., Hatcher, E., Acharya, C., Kundu, S., Zhong, S., Shim, J., Darian, E., Guvench, O., Lopes, P., Vorobyov, I., Mackerell, A. D., Jr., CHARMM general force field: A force field for drug-like molecules compatible with the CHARMM all-atom additive biological force fields. *J Comput Chem.* 2010; 31(4): 671-90.
60. Aier, I., Varadwaj, P. K., Raj, U., Structural insights into conformational stability of both wild-type and mutant EZH2 receptor. *Sci Rep*. 2016; 6: 34984.
61. Roccatano, D., Colombo, G., Fioroni, M., Mark, A. E., Mechanism by which 2,2,2-trifluoroethanol/water mixtures stabilize secondary-structure formation in peptides: a molecular dynamics study. *Proc Natl Acad Sci U S A.* 2002; 99(19): 12179-84.
62. Lobanov, M., Bogatyreva, N. S., Galzitskaia, O. V., [Radius of gyration is indicator of compactness of protein structure]. *Mol Biol (Mosk).* 2008; 42(4): 701-6.
63. Mazola, Y., Guirola, O., Palomares, S., Chinea, G. Menéndez, C., Hernández, L., Musacchio, A., A comparative molecular dynamics study of thermophilic and mesophilic β-fructosidase enzymes. *J Mol Model.* 2015, 21(9), 228.
64. Antunes, D. A., Rigo, M. M., Sinigaglia, M., de Medeiros, R. M., Junqueira, D. M., Almeida, S. E., Vieira, G. F., New insights into the in silico prediction of HIV protease resistance to nelfinavir. *PLoS One.* 2014; 9(1): e87520.
65. Panigrahi, S. K., Strong and weak hydrogen bonds in protein-ligand complexes of kinases: a comparative study. *Amino Acids.* 2008; 34(4): 617-33.
66. Junior, A. G., Gasparotto, F. M., Boffo, M. A., Lourenço, E. L. B., Stefanello, M. É. A., Salvador, M. J., da Silva-Santos, J. E., Marques, M. C. A., Kassuya, C. A. L., Diuretic and potassium-sparing effect of isoquercitrin—An active flavonoid of Tropaeolum majus L. *Journal of Ethnopharmacology*. 2011; 134(2): 210-215.

67. Bhavin, V., Ruchi, V., Santani, D., Diuretic potential of whole plant extracts of Pergularia daemia (Forsk.). *Iranian Journal of Pharmaceutical Research: IJPR*. 2011; 10(4): 795.
68. Feng, Y.-L., Lei, P., Tian, T., Yin, L., Chen, D.-Q., Chen, H., Mei, Q., Zhao, Y.-Y., Lin, R.-C., Diuretic activity of some fractions of the epidermis of Poria cocos. *Journal of Ethnopharmacology*. 2013; 150(3): 1114-1118.
69. Amuthan, A., Chogtu, B., Bairy, K., Prakash, M., Evaluation of diuretic activity of Amaranthus spinosus Linn. aqueous extract in Wistar rats. *Journal of ethnopharmacology*. 2012; 140(2): 424-427.
70. Ntchapda, F., Barama, J., Azambou, D. R. K., Etet, P. F. S., Dimo, T., Diuretic and antioxidant activities of the aqueous extract of leaves of Cassia occidentalis (Linn.) in rats. *Asian Pacific Journal of Tropical Medicine*. 2015; 8(9): 685-693.
71. Tirumalasetty, J., Chandrasekhar, N., Naveen, A., Evaluation of diuretic activity of ethanol extract of Benincasa hispida stem in Swiss albino rats. *Journal of Chemical and Pharmaceutical Research.* 2013; 5(3): 91-97.
72. de AF Da, R. d. C., de Souza, P., Crestani, S., Júnior, A. G., Boligon, A. A., Athayde, M. L., da Silva-Santos, J. E., Hypotensive and diuretic effect of the butanolic soluble fraction of the hydroethanolic extract of bark of Scutia buxifolia Reissek in rats. *Journal of ethnopharmacology*. 2015; 172: 395-401.
73. Kumar, B. S., Swamy, B. V., Archana, S., Anitha, M., A review on natural diuretics. *Research Journal of Pharmaceutical, Biological and Chemical Sciences*. 2010; 1(4): 615-634.
74. Biswas, B., Golder, M., Abid, M. A., Mazumder, K., Sadhu, S. K., Terpenoids enriched ethanol extracts of aerial roots of Ceriops decandra (Griff.) and Ceriops tagal (Perr.) promote diuresis in mice. *Heliyon*. 2021; 7(7): e07580.
75. KP, S. G., CM, M., Kumar, V., Study on the diuretic :activity of Cynodon dactylon root stalk extract in albino rats. *Research Journal of Pharmacy and Technology*. 2009; 2(2): 338-340.
76. Martin-Herrera, D., Abdala, S., Benjumea, D., Gutierrez-Luis, J., Diuretic activity of some Withania aristata Ait. fractions. *Journal of ethnopharmacology*. 2008; 117(3): 496-499.
77. Alarcón-Alonso, J., Zamilpa, A., Aguilar, F. A., Herrera-Ruiz, M., Tortoriello, J., Jimenez-Ferrer, E., Pharmacological characterization of the diuretic effect of Hibiscus sabdariffa Linn (Malvaceae) extract. *Journal of Ethnopharmacology*. 2012; 139(3): 751-756.
78. Moser, J. C., Cechinel-Zanchett, C. C., Mariano, L. N. B., Boeing, T., da Silva, L. M., de Souza, P., Diuretic, natriuretic and Ca2+-sparing effects induced by rosmarinic and caffeic acids in rats. *Revista Brasileira de Farmacognosia*. 2020; 30(4): 588-592.
79. Kurkin, V., Zaitseva, E., Kurkina, A., Dubishchev, A., Pravdivtseva, O., Comparative study of diuretic activity of hydroalcoholic extracts from medicinal plants containing flavonoids. *Bulletin of experimental biology and medicine*. 2015; 159(3): 368-372.

تقييم خاصية مدر للبول من Argemone mexicana مع دراسة الالتحام الجزيئي

بابيترا كومار سردار[1]، هيرون سراج ديفناث[1]، نريبندرا ناث بيسواس[1*]، بيشواجيت بوكشي[1*]، سمير كومار سادو[1]

[1] تخصص الصيدلة، كلية علوم الحياة، جامعة خولنا، خولنا –9208، بنغلاديش.

ملخص

الخلفية: تم استخدام Argemone mexicana L. (A. mexicana) تقليديًا لعلاج ارتفاع ضغط الدم ومشاكل المسالك البولية والإمساك. هنا، تم تقييم مستخلص الخام الإيثانولي A. mexicana للنشاط المدر للبول.

الطريقة: تم إجراء الاختبارات الكيميائية النباتية باستخدام الكواشف والطرق القياسية المقبولة عمومًا. تم إجراء اختبار مدر للبول في أقفاص أيضية باستخدام نموذج الفئران حيث تم أخذ فوروسيميد (5 مجم / كجم) كدواء قياسي. تم إجراء عملية الالتحام الجزيئي في PyRx باستخدام autodock vina 4.2. لتقييم ثبات مجمع بروتين–يجند الراسي، تم إجراء محاكاة الديناميكيات الجزيئية (MD) لمركب البروتين β-amyrin-6PZT ومركب بروتين فوروسيميد –6 PZT. تم حساب قيم RMSD و RMSF و Rg و SASA والروابط الهيدروجينية لجميع مجمعات البروتين – الترابط.

النتائج: أظهر الفحص الكيميائي النباتي وجود قلويدات، فلافونويد، جليكوسيدات، منشطات، تربينويد، صابونين، وتانينات. أظهر المستخلص الخام نشاطا مدر للبول معنويا ($P < 0.05$) مقارنة مع المجموعة الضابطة. علاوة على ذلك، تم الكشف عن وجود إلكتروليتات+ Na) ، + K، و Cl) في بول الفئران المعالجة بالمستخلص الخام. في دراسة الالتحام الجزيئي، من بين المركبات الثمانية عشر المبلغ عنها، وجد β-amyrin قدرة فائقة على إدرار البول. أظهرت نتيجة محاكاة الديناميكيات الجزيئية لمركب البروتين β-amyrin-6PZT استقرارًا جيدًا مقارنة بالفوروسيميد المرجعي.

الخلاصة: المستخلص الخام من A. mexicana له تأثيرات مدرة للبول يمكن استخدامها لعلاج الوذمة. قد تساعد نتيجة الالتحام الجزيئي ومحاكاة الديناميكيات الجزيئية في إجراء مزيد من الدراسات لتطوير دواء جديد.

الكلمات الدالة: Argemone mexicana، Papaveraceae، مدر للبول، الالتحام الجزيئي، β-amyrin.

* ***المؤلف المراسل:***

نريبندرا ناث بيسواس: nnathbiswas@gmail.com

بيشواجيت بوكشي: bokshi06@pharm.ku.ac.bd

تاريخ استلام البحث 2022/9/19 وتاريخ قبوله للنشر 2023/4/28.